

Multilayer adsorption and wetting: Ethylene on graphite

M. Drir, H. S. Nham, and G. B. Hess

Physics Department, University of Virginia, Charlottesville, Virginia 22901

(Received 24 December 1985)

An ellipsometric technique was used to measure a set of adsorption isotherms for ethylene on a single cleaved surface of graphite in the vicinity of the triple point ($T_3 = 104$ K) of ethylene. At least seven or eight discrete layers are observed at temperatures slightly above T_3 , contrary to a previous suggestion of a prewetting transition after two monolayers. Evidence is presented that this layered liquid film becomes unstable with respect to bulk liquid at about ten layers, so that wetting is incomplete even above T_3 .

The earliest multilayer physisorption measurements with substrates sufficiently uniform to produce stepped isotherms showed layer-by-layer growth approaching the bulk solid phase of the adsorbate. This is true for xenon, krypton, argon, and methane on graphite,^{1,2} and is referred to as "type 1" or Frank-van der Merwe growth, or complete wetting.³ Subsequent work has shown that this is actually the exceptional case, requiring a fairly delicate balance between the adsorbate-adsorbate molecular attraction and the adsorbate-substrate attraction; outside a limited range, a bulk solid adsorbate appears in equilibrium with a film only a few molecular layers thick.⁴⁻¹⁰ This is called "type 2" or Stranski-Krastanov growth, or incomplete wetting.^{3,11} Above the triple point where the bulk phase of the adsorbate is liquid, complete wetting has been found in nearly every case studied in physisorption experiments.¹² Pandit and Fisher¹³ have discussed possible multilayer phase diagrams in the neighborhood of the bulk triple point, T_3 . The measurements reported here support their suggestion that, for ethylene on graphite in the region below T_3 , the bulk solid simply preempts the liquid film beyond some thickness.

The system ethylene on graphite provided the first recognized example of a wetting transition. In volumetric isotherm measurements, Menaucourt, Thomy, and Duval⁴ reported the appearance of a second layer at 80 K and a third layer at 98 K. Although no further steps were resolved, the coverage on isotherms above 104 K appeared to diverge approaching the saturated vapor pressure P_0 , indicating complete wetting. Bassignana and Larher¹⁴ found a fourth step, appearing above about 102 K. Similar results were reported on boron nitride and PbI_2 substrates.^{14,15} In x-ray diffraction measurements, Sutton and co-workers¹⁶ confirmed the coexistence of bulk solid successively with one-, two-, and three-layer films on increasing temperature. Resolving no further layers approaching T_3 at high coverage, they suggested that the third step may represent a prewetting transition, beyond which the film grows continuously. We will show this is not the case. The difficulty in all of these experiments in observing higher steps, and also in determining unambiguously whether wetting occurs, is due to capillary condensation between flakes of the exfoliated (or powder) substrate, which becomes important at pressures above about $0.9P_0$.

In this paper we report adsorption measurements on a single cleaved surface of highly oriented pyrolytic graphite (HOPG).¹⁷ This eliminates the possibility of capillary condensation, while providing a surface with larger facet size and better energy uniformity than exfoliated graphites. We

measure adsorbate coverage by a phase-modulation ellipsometric technique,¹⁸ using laser light reflected from a $0.1 \times 0.2\text{-mm}^2$ spot on the graphite surface.

For a transparent, plane-parallel film on a flat substrate, any ellipsometer output is a periodic function of film thickness. For an ethylene film and a 45° angle of incidence, the period corresponds to roughly 700 molecular layers. For films much thinner than this, our ellipsometer provided an output I_1 (the component of intensity at the modulation frequency) which is directly proportional to coverage. A second output I_2 (the component of intensity at twice the modulation frequency) varies roughly in quadrature with I_1 , and so is useful in following the growth of thicker films. Both these outputs are normalized to the dc intensity I_0 . I_0 also provides an indication of macroscopic (on the order of the wavelength) nonuniformity of the film, which leads to scattering out of the specular beam.

The HOPG sample is mounted in an ion-pumped stainless-steel cell containing two windows 90° apart. The entire cell and the capacitance pressure gauge are maintained at low temperature, up to a room-temperature valve at the pumping manifold. The sample is mounted on a cold finger which is temperature regulated at a few degrees colder than the cell body. There is also separate temperature control of a copper baffle.

The initial isotherm of a run is recorded while admitting ethylene gas to the cell through a leak valve. Subsequently the pressure is lowered by cooling the baffle well below the temperature of the sample, and raised again by heating the baffle. In this way we can cycle the coverage on the sample from one to two layers at minimum to macroscopic coverage at saturation. The sample does not remain exactly isothermal, but the deviation is small until the start of bulk condensation.¹⁹

A sequence of ellipsometric isotherms between 99 and 108 K, each starting after the second layer, is shown in Fig. 1. The abscissa for each isotherm has been normalized by P_n^* , the pressure extrapolated to infinite thickness according to the Frankel-Halsey-Hill equation,²⁰

$$k_B T \ln(P_n / P_n^*) = \mu_n - \mu_\infty^* = -\alpha n^{-3}, \quad (1)$$

where n is the number of layers, P_n (or μ_n) is the pressure (or chemical potential) during n th-layer condensation, and α is proportional to the van der Waals constant. With this normalization, the chemical potential of isotherms above and below the triple point are referred to a common reference state (hypothetical layered liquid). The isotherms

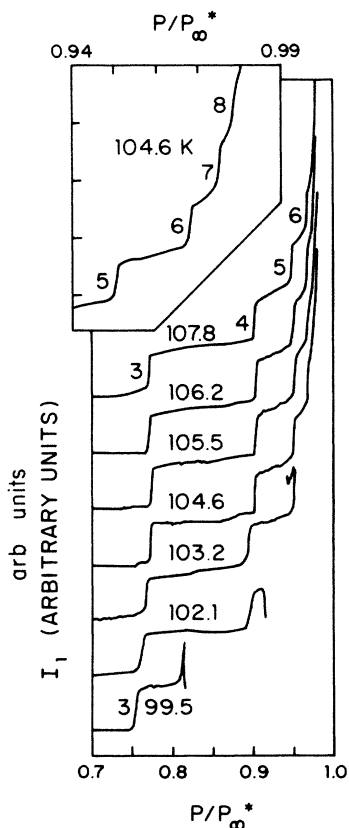


FIG. 1. Ethylene coverage vs reduced pressure at seven temperatures (labeled). The portion of the isotherms shown here begins after two layers, and succeeding layer step numbers are indicated. Below the triple point ($T < 104$ K) the isotherms terminate with rapid oscillation of the signal, truncated here. Above 104 K they rise to the equivalent of about 50 layers. The inset shows part of one isotherm with expanded abscissa.

below T_3 terminate with the appearance of three-dimensional crystallites, which is indicated by the onset of rapid fluctuations in I_1 and a rapid decrease in I_0 , which falls usually to less than 3% of its initial value. Above T_3 , the coverage signal I_1 increases to the equivalent of about 50 layers. As can be seen in the inset in Fig. 1, at least eight steps can be resolved, which, although not necessarily vertical, at least represent a strong modulation of the isotherm. The behavior beyond eight layers will be discussed later.

From the pressures at the steps in 17 isotherms, including those in Fig. 1, we can find the loci of layer condensation in the μ - T plane. These data are shown in Fig. 2. The solid lines are fit to the observed bulk condensation points.

The first observation is that the layer lines are horizontal within experimental error. This is true also for the second layer, not shown. This implies that the partial molar entropy of the film at each layer condensation is equal to the bulk liquid entropy, with an uncertainty of $0.1k_B$ (except for the second layer where it is $0.5k_B$). In this sense the film is liquidlike; indeed, the known melting points of the first layer (95 K)^{21,22} and the second layer (94 K)¹⁶ are below the range of these measurements. The higher layers are apparently preempted by the bulk solid before two-dimensional (2D) solidification.

Since the layer lines are horizontal, we estimate the

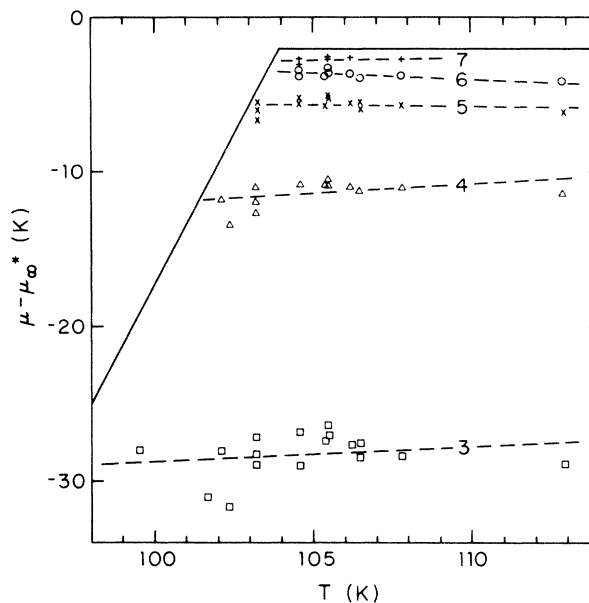


FIG. 2. Loci of layer steps 3-7 in the variables temperature and chemical potential, from 17 measured isotherms. The solid lines are fit to the appearance of the bulk phase.

chemical potential at condensation of the n th layer ($n = 3-7$), relative to the bulk liquid, by averaging data for seven isotherms above T_3 .²³ These averages are listed in column 2 of Table I. The saturated vapor pressure P_0 is identified by the beginning of the decrease in I_0 and by a simultaneous break in the rate of increase of pressure.²⁴

The chemical potential of the film can be compared to simple theoretical estimates. The chemical potential of bulk liquid in equilibrium with vapor differs from that of the film in that (a) the substrate is replaced by an extended liquid adsorbate in calculating the attractive potential and (b) the structure of the film and the bulk, and hence their internal energies, may be different. The essence of the Frankel-Halsey-Hill (FHH) model is that the second contribution is neglected,²⁰ and we provisionally make this approximation. The potential of the substrate is often approximated by

$$V_S(z) = -C_{3s}/z^3, \tag{2}$$

where C_{3s} is the van der Waals coefficient of the graphite

TABLE I. Chemical potential of film during condensation of the n th layer, relative to bulk liquid, and residuals of fits described in the text. The entries are in temperature units.

n	$\mu_n - \mu_0$ (K)	Residuals: $\mu_n - \mu_n(\text{fit})$ (K)	
		Eq. (1)	Eq. (7)
2	-99.43 ± 2.45	-10.47	-1.77
3	-25.41 ± 0.92	-0.53	1.16
4	-8.72 ± 0.19	0.59	0.05
5	-3.40 ± 0.23	0.36	-0.25
6	-1.54 ± 0.25	-0.23	-0.03
7	-0.67 ± 0.19	-0.61	0.10
(Sat.)	0 ± 0.34		
$\mu_\infty - \mu_0$		(2.1 ± 0.4)	1.0 ± 0.4
α		(727 ± 13)	458 ± 8

substrate (C_{3a} will be the corresponding coefficient for the bulk adsorbate) and $z = nd$ is the distance of an adsorbate atom in the n th layer from the substrate surface, with d the thickness of a monolayer of adsorbate. ($z = 0$ is the plane of the centers of the carbon atoms in the top graphite layer.) Then the FHH model leads to Eq. (1) with

$$\alpha = (C_{3s} - C_{3a})/d^3. \quad (3)$$

We have made a least-squares fit of Eq. (1) to the data. The resulting values of α and μ_∞ , together with the residuals $\mu_n(\text{expt}) - \mu_n(\text{fit})$, are given in column 3 of Table I. We do not use the saturation point ($P_\infty/P_0 = 1$) in the fit, or force $P_\infty = P_0$, because there is the possibility of a physical difference between P_0 and P_∞ , as is discussed below.

Equation (2) is seriously inaccurate for small z . A better approximation is obtained by evaluating the discrete sum over layers of the van der Waals potential due to successive graphite layers below the interface.²⁵ The resulting potential for the n th adsorbate layer can be written in the form

$$V_{S,n} = -C_{3s}d^{-3}(n - \beta_n)^{-3}, \quad (4)$$

where β_n is obtained by numerical summation or by using the approximation²⁵

$$\beta_n = 0.5 - 0.186(nd/d_1)^{-1} + 0.02(nd/d_1)^{-2}, \quad (5)$$

where $d_1 = 3.35 \text{ \AA}$ is the graphite layer spacing. The value of d for the liquid film is not known, and must be estimated from the bulk liquid density and some assumption about the structure of the film. (We take $d/d_1 = 1.20$ for ethylene.) Treatment of the bulk liquid adsorbate reference state is more problematic, since it is unlayered, and it might be appropriate to take $\beta_n = \frac{1}{2}$. However, in the context of the FHH model, it is unlikely a serious error will result if the same β_n values are used as for graphite. With this approximation, Eq. (1) is replaced by

$$\mu_n - \mu_\infty = -\alpha(n - \beta_n)^{-3} \quad (6)$$

with α still given by Eq. (3).

A fit of this equation to our experimental data is given in column 4 of Table I. Since deficiencies of the model should be most severe for the thinnest films, we repeated the fit excluding the $n = 2$ datum, but found little change ($\alpha = 466 \text{ K}$, $\mu_\infty - \mu_0 = 1.0 \text{ K}$). The result that $\mu_\infty > \mu_0$ implies that the layered film has slightly greater internal energy than isotropic liquid and that wetting is incomplete. Indeed, droplet condensation appears in coincidence approximately with a 10-layer film, consistent with the extrapolated chemical potential difference.

Finally, we discuss evidence on the growth behavior of thicker films, where layers are not resolved, for temperatures above T_3 . The normalized coverage signal I_1 continues to increase to the equivalent of about 50 layers, as we have mentioned, and then levels off or begins to decrease. Beyond about 10 layers the dc output I_0 begins to decrease, indicating scattering by droplets. This decrease accelerates, until abruptly I_0 levels off at about 55% of its initial value

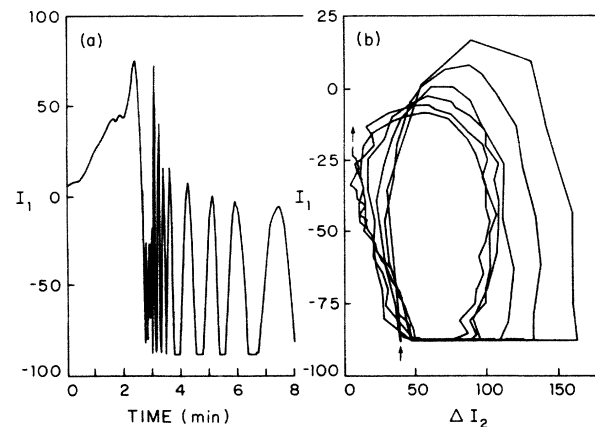


FIG. 3. An isotherm at 104.3 K, extending to large coverage: (a) Coverage signal I_1 vs time. There are already eight layers at time $t = 0$. (b) I_1 vs quadrature signal I_2 , for the regular oscillatory part of the isotherm, between $t = 3.5$ and 11 min. The six cycles shown here correspond to film growth by about $1.7 \mu\text{m}$. The units of I_1 correspond to monolayers at low coverage. The I_1 channel saturates at -88 units.

and then oscillates about this level as long as the film is in saturation. Coincident with the rapid drop of I_0 , I_1 also decreases rapidly to a negative value, about which it then oscillates. [In the example given in Fig. 3(a), the oscillation is somewhat larger and more regular than is typical.] The negative mean value is consistent with incoherent reflections from the front and back surfaces of the film. We interpret these observations to mean the film has become macroscopically thick and wavy or patchy. This interpretation is supported by the observation of oscillations in I_2 in the proper phase relation to I_1 . This is shown in the Lissajous pattern of Fig. 3(b), which has the shape expected for film growth through multiple periods. The same behavior is seen in reverse on evaporation, except the peak value of I_1 is smaller (about 30 apparent layers) and there is a delay in the complete recovery of I_0 to its initial value. We believe that, between 10 and 50 apparent layers, the film actually consists of droplets of size increasing with time, distinguishable from a uniform film by I_0 but not I_1 . The subsequent rapid transition may involve growth of droplets to wavelength dimensions, coalescence into a thick film, and possibly subsequent flow, such as sagging under gravity, or some kinetic instability.

Finally, we remark that the present results are very similar to those for oxygen, near its triple point, on graphite.²⁶

We have benefited from discussions with M. W. Cole, M. H. W. Chan, J. G. Dash, and S. E. Schnatterly, and are grateful for the assistance of H. S. Youn, M. Lambertson, and J. Shields with various aspects of this experiment. This work was supported by the Low Temperature Physics program of the National Science Foundation under Grant No. DMR81-16922.

¹A. Thomy and X. Duval, *J. Chim. Phys.* **66**, 1966 (1969); **67**, 286 (1970).

²H. M. Kramer, *J. Cryst. Growth* **33**, 65 (1976); G. L. Price and J. A. Venables, *Surf. Sci.* **49**, 264 (1975).

³J. G. Dash, *Phys. Rev. B* **15**, 3136 (1977); R. Pandit, M. Schick, and M. Wortis, *ibid.* **26**, 5112 (1982).

⁴J. Menaucourt, A. Thomy, and X. Duval, *J. Phys. (Paris) Colloq.* **38**, C4-195 (1977).

- ⁵J. L. Seguin, J. Suzanne, M. Bienfait, J. G. Dash, and J. A. Venables, *Phys. Rev. Lett.* **51**, 122 (1983).
- ⁶M. Bienfait, J. L. Seguin, J. Suzanne, E. Lerner, J. Krim, and J. G. Dash, *Phys. Rev. B* **29**, 983 (1984).
- ⁷J. Venables, J. L. Seguin, J. Suzanne, and M. Bienfait, *Surf. Sci.* **145**, 345 (1984).
- ⁸J. Krim, J. G. Dash, and J. Suzanne, *Phys. Rev. Lett.* **52**, 640 (1984).
- ⁹A. D. Migone, J. Krim, J. G. Dash, and J. Suzanne, *Phys. Rev. B* **31**, 7643 (1985).
- ¹⁰R. J. Muirhead, J. G. Dash, and J. Krim, *Phys. Rev. B* **29**, 5074 (1984).
- ¹¹For a recent review from an experimental point of view, see M. Bienfait, *Surf. Sci.* **162**, 411 (1985).
- ¹²An exception is reported by Migone *et al.*, Ref. 9, in the case of helium on Au(111) and Ag(111), for which an explanation is proposed by J. Krim and J. G. Dash, *Surf. Sci.* **162**, 421 (1985).
- ¹³R. Pandit and M. E. Fisher, *Phys. Rev. Lett.* **51**, 1772 (1983).
- ¹⁴I. C. Bassignana and Y. Larher, *Surf. Sci.* **147**, 48 (1984).
- ¹⁵C. Bockel, J. Menucourt, and A. Thomy, *J. Phys. (Paris)* **45**, 1391 (1984).
- ¹⁶M. Sutton, S. G. J. Mochrie, and R. J. Birgeneau, *Phys. Rev. Lett.* **51**, 407 (1983); S. G. J. Mochrie, M. Sutton, R. J. Birgeneau, D. E. Moncton, and P. M. Horn, *Phys. Rev. B* **30**, 263 (1984).
- ¹⁷HOPG is a product of Union Carbide Corporation.
- ¹⁸The configuration is similar to case b of S. N. Jaspersen and S. E. Schnatterly, *Rev. Sci. Instrum.* **40**, 761 (1969), with a quarter-wave compensator added.
- ¹⁹The largest resulting pressure correction during layer condensation is 0.5%.
- ²⁰See W. A. Steele, *The Interaction of Gases with Solid Surfaces* (Pergamon, Oxford, 1974), p. 238ff.
- ²¹J. Z. Larese and R. J. Rollefson, *Surf. Sci.* **127**, L172 (1983).
- ²²H. K. Kim, Q. M. Zhang, and M. H. W. Chan (unpublished); M. K. Kim, Ph.D. thesis, Pennsylvania State University, 1985 (unpublished).
- ²³Since not all isotherms extend to the second step, we include data from slightly below T_3 for $n = 2$.
- ²⁴A third indication of heavy condensation on the sample mount is the beginning of an increase in its temperature. However, this is delayed several seconds due to the external location of the thermometer.
- ²⁵S. Chung, N. Holter, and M. W. Cole, *Phys. Rev. B* **31**, 6660 (1985), Appendix.
- ²⁶M. Drir and G. B. Hess, *Phys. Rev. B* **33**, 4758 (1986).